

# Role of projection in the control of bird flocks

Daniel J. G. Pearce<sup>a,b</sup>, Adam M. Miller<sup>a,c</sup>, George Rowlands<sup>a</sup>, and Matthew S. Turner<sup>a,c,d,1</sup>

Departments of <sup>a</sup>Physics and <sup>b</sup>Chemistry and <sup>c</sup>Centre for Complexity Science, University of Warwick, Coventry CV4 7AL, United Kingdom; and <sup>d</sup>Laboratoire Physico-Chimie Théorique, Gulliver, Centre National de la Recherche Scientifique, Unité Mixte de Recherche 7083, Ecole Supérieure de Physique et de Chimie Industrielles, 75231 Paris Cedex 05, France

Edited by Paul M. Chaikin, New York University, New York, NY, and approved May 19, 2014 (received for review February 7, 2014)

**Swarming is a conspicuous behavioral trait observed in bird flocks, fish shoals, insect swarms, and mammal herds. It is thought to improve collective awareness and offer protection from predators. Many current models involve the hypothesis that information coordinating motion is exchanged among neighbors. We argue that such local interactions alone are insufficient to explain the organization of large flocks of birds and that the mechanism for the exchange of long-range information necessary to control their density remains unknown. We show that large flocks self-organize to the maximum density at which a typical individual still can see out of the flock in many directions. Such flocks are marginally opaque—an external observer also still can see a substantial fraction of sky through the flock. Although this seems intuitive, we show it need not be the case; flocks might easily be highly diffuse or entirely opaque. The emergence of marginal opacity strongly constrains how individuals interact with one another within large swarms. It also provides a mechanism for global interactions: an individual can respond to the projection of the flock that it sees. This provides for faster information transfer and hence rapid flock dynamics, another advantage over local models. From a behavioral perspective, it optimizes the information available to each bird while maintaining the protection of a dense, coherent flock.**

flocking | collective motion

Starling murmurations represent one of the most impressive examples of organization in the natural world, with flocks of up to 300,000 individuals or more able to coordinate themselves into a cohesive and highly coherent group (1–5).

Although the primary source of sensory information to a bird is visual, it would be unrealistic to expect that individual to recognize and track the position and orientation of a significant proportion of the other members of a flock (3, 4). Indeed, observations on real starling flocks show that a bird responds to this type of information only from its seven nearest neighbors and that these interactions are scale-free (1, 5, 6). Local interactions such as this are enough to create order within a flock (5–10) but do not give any information on the state of the flock as a whole, nor do they explain how density might be regulated. Most models use attraction and repulsion interactions, use a fictitious potential field, or simply fix the available volume to control the density (6–8, 11–20).

To make progress, we first ask a simple question: “What does a bird actually see when it is part of a large flock?” Its view out from within a large flock likely would present the vast majority of individuals merely as silhouettes, moving too fast and at too great a distance to be tracked easily or even discriminated from one another. Here the basic visual input to each individual is assumed to be based simply on visual contrast: a dynamic pattern of dark (bird) and light (sky) across the field of vision (although it might be possible to extend this to other swarming species and environmental backgrounds, respectively). This has the appealing feature that it also is the projection that appears on the retina of the bird, which we assume to be its primary sensory input. A typical individual within a very dense flock would see other, overlapping individuals (dark) almost everywhere it looked. Conversely, an isolated individual, detached from the flock, would see only sky (light). The projected view gives direct

information on the global state of the flock. It is a lower-dimensional projection of the full  $6N$  degrees of freedom of the flock and therefore is more computationally manageable, both for the birds themselves and for the construction of simple mathematical models of swarm behavior.

The information required to specify the projection mathematically is linear in the number of boundaries. Our simplifying assumption is that the individual registers only such a black-and-white projection (in addition to nearest-neighbor orientation). This information, then, is all that would be available to an agent, regardless of the behavioral model that might be chosen. Individuals in a flock that is sparse enough for them to typically see a complex projected pattern of dark and light have more information about the global state of the flock. Such sparse flocks also allow an individual to see out in a significant fraction of all directions, which would allow the approach of a predator, or at least the response of distant individuals to the approach of a predator, to be registered. Conversely, a dense, completely opaque flock would offer little information about either the global state of the flock or the approach of predators.

We define the opacity,  $\Theta'$ , of a flock to be the fraction of sky obscured by individuals from the viewpoint of a distant external observer. A closely related quantity is the average opacity seen by a typical individual located within the flock, written  $\Theta$ . Crucially, the opacity and density are quite different quantities: flocks containing large numbers of individuals might be nearly opaque ( $\Theta \sim 1$ ) even for very small densities, corresponding to well-separated birds. Below we present evidence that large bird flocks are marginally opaque, with opacities that are intermediate, neither very close to 0 nor 1 ( $0.25 \lesssim \Theta' \lesssim 0.6$  in our data). Such a state corresponds to a complex projected pattern rich in information.

## Significance

**We propose a new model for long-range information exchange in bird flocks based on the projected view of each individual out through the flock. Visual input is coarse grained to a pattern of (dark) bird against (light) sky. We propose the simplest hybrid projection model that combines metric-free coalignment, and noise, with this projected view; here the birds fly toward the resolved vector sum of all the domain boundaries. This model leads to robustly coherent flocks that self-assemble to a state of marginal opacity. It therefore provides a mechanism for the control of density. Although it involves only two primary control parameters, it also gives rise to several distinct phenotypes. We compare our predictions with experimental data.**

Author contributions: D.J.G.P., G.R., and M.S.T. designed research; D.J.G.P. and A.M.M. performed research; D.J.G.P., A.M.M., and M.S.T. contributed new reagents/analytic tools; D.J.G.P., A.M.M., G.R., and M.S.T. analyzed data; and D.J.G.P., A.M.M., and M.S.T. wrote the paper.

The authors declare no conflict of interest.

This article is a PNAS Direct Submission.

<sup>1</sup>To whom correspondence should be addressed. Email: m.s.turner@warwick.ac.uk.

This article contains supporting information online at [www.pnas.org/lookup/suppl/doi:10.1073/pnas.1402202111/-DCSupplemental](http://www.pnas.org/lookup/suppl/doi:10.1073/pnas.1402202111/-DCSupplemental).

In the remainder of this article, we focus on proposing a model for how bird flocks organize and specifically on how the global density is regulated, which remains an open question (1). We develop what we believe to be the simplest possible model that takes the projected view described above as sensory input while retaining coalignment with (visible) nearest neighbors and allowing for some noise. We then compare the swarms generated by this model with data.

### Hybrid Projection Model

We propose a hybrid projection model in which each individual responds to the projection through the swarm it observes. We first identify those (dark) angular regions in which a line of sight traced from an individual to infinity intersects one or more other members of the swarm. These are separated by (light) domains (Fig. 1).

Each individual is assumed to be isotropic and has a size  $b = 1$ , which then defines our units of length. Anisotropic bodies give rise to a projected size that depends on orientation and are explored further in *SI Appendix*. In two dimensions, the domain boundaries seen by the  $i^{\text{th}}$  individual define a set of angles  $\theta_{ij}$ , measured from an arbitrary reference ( $x$ ) axis, where the index  $j$  runs over all the  $\mathcal{N}_i$  light–dark (or dark–light) domain boundaries seen by the  $i^{\text{th}}$  individual, equal to 10 for the central individual shown in Fig. 1. These  $\theta_{ij}$  are a reasonable choice for input to a behavioral model: edge detection such as this is known to be performed in the neural hardware of the visual cortex in higher animals (21). In particular, behavioral models based on motional bias toward either the most dark or light regions tend to be unstable with respect to collapse or expansion, respectively. The simplest candidate model that might support physically reasonable solutions therefore is one that responds to the domain boundaries. We seek a model that takes as input the angles specifying the domain boundaries and produces a characteristic direction for the birds, acknowledging that their actual motion also should include their known tendency to coalign with neighbors and also the effect of some noise. A natural choice for this characteristic direction is simply the average direction to all boundaries  $\underline{\delta}_i$ :

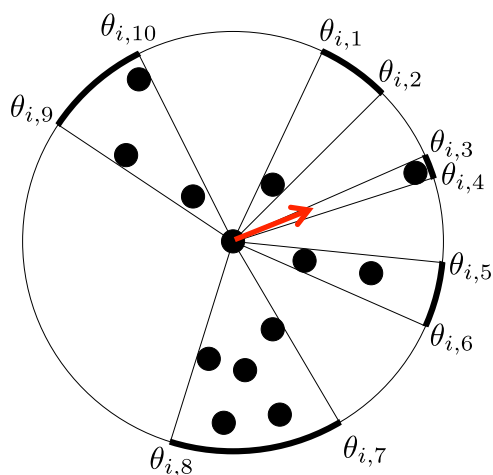


**Fig. 1.** Sketch showing the construction of the projection through a 2D swarm seen by the  $i^{\text{th}}$  individual, which here happens to be one near the center of the swarm. The thick dark arcs around the exterior circle (shown for clarity; there is no such boundary around the swarm) correspond to the angular regions where one or more others block the line of sight of the  $i^{\text{th}}$  individual to infinity. The sum of unit vectors pointing to each of these domain boundaries, at the angles shown, gives the resolved vector  $\underline{\delta}_i$ , shown in red, that enters our equation of motion. See *SI Appendix* for the extension to 3D.

$$\underline{\delta}_i = \frac{1}{\mathcal{N}_i} \sum_{j=1}^{\mathcal{N}_i} \begin{pmatrix} \cos \theta_{ij} \\ \sin \theta_{ij} \end{pmatrix}. \quad [1]$$

This easily can be extended to 3D flocks, in which the light–dark boundaries now may be represented as curves on the surface of a sphere and  $\underline{\delta}$  becomes the normalized integral of radial unit vectors traced along these curves; see *SI Appendix* for details.

Our model involves  $\underline{\delta}_i$  in such a way as to correspond to birds being equally attracted to all the light–dark domain boundaries. In addition, they coalign with visible local neighbors, assigned in a topological fashion (6, 9). We define visible neighbors to be those for which there is an unbroken line of sight between the two individuals (see *SI Appendix* for details). We incorporate these two preferred directions, arising from the projection and the motion of neighbors, into an otherwise standard agent-based model for a swarm of  $N$  particles moving off-lattice with constant speed  $v_0$  ( $v_0 = 1$  in all our simulations). For simplicity, we treat the individuals as “phantoms,” having no direct steric interactions (the effect of introducing steric interactions is explored further in *SI Appendix*). The equation of motion for the position  $\underline{r}_i^t$  of the  $i^{\text{th}}$  individual at discrete time  $t$  is

$$\underline{r}_i^{t+1} = \underline{r}_i^t + v_0 \underline{v}_i^t \quad [2]$$

with a velocity parallel to

$$\underline{v}_i^{t+1} = \phi_p \underline{\delta}_i^t + \phi_a \langle \widehat{\underline{v}}_k^t \rangle_{n,n} + \phi_n \underline{\eta}_i^t, \quad [3]$$

where  $\langle \dots \rangle_{n,n}$  is an average over the  $k \in [1, \sigma]$  nearest neighbors to the  $i^{\text{th}}$  individual ( $\sigma = 4$  in all simulations); a hat ( $\widehat{\phantom{x}}$ ) denotes a normalized vector; and  $\underline{\eta}_i^t$  is a noise term of unit magnitude having a different (uncorrelated) random orientation for each individual at each timestep. This equation involves only three primary control parameters,  $\phi_p$ ,  $\phi_a$ , and  $\phi_n$ , the weights of the projection, alignment, and noise terms, respectively. We further simplify by considering only the relative magnitudes (ratios) of these control parameters, which then are taken to obey

$$\phi_p + \phi_a + \phi_n = 1. \quad [4]$$

We now analyze the results of computer simulation of the swarms arising from these equations of motion for given combinations of  $\{\phi_p, \phi_a\}$  alone, with  $\phi_n$  given by construction through Eq. 4. Several distinct behavioral phenotypes reminiscent of birds, fish, and insects are observed (*Movies S1, S2, and S3*, respectively). Further generalizations of the model also are explored in *SI Appendix*, including the effect of steric/repulsive interactions and incomplete angular vision corresponding to “blind angles” behind each bird (*Movies S4–S6*).

### The Hybrid Projection Model Reproduces Key Features of a Flock of Birds

In particular, it naturally leads to robustly cohesive swarms (Fig. 2*A* and *B* and *SI Appendix*) as well as the emergence of marginal opacity in large flocks of birds in which both  $\Theta$  and  $\Theta'$  are neither very close to 0 nor 1 (Fig. 2*C* and *D*).

The emergence of marginal opacity is a new feature, and it is worth emphasizing that the model was not constructed so as to target any particular “preferred” opacity value; rather, marginal opacity emerges naturally. Importantly, it arises for swarms of varying size  $N$  that are realized with exactly the same control parameters  $\phi_p$  and  $\phi_a$ . This means that marginal opacity can be maintained without a bird changing its behavior with, or even being aware of, the size of the flock. Other models, which control the density in a metric fashion (11, 14), give rise to values

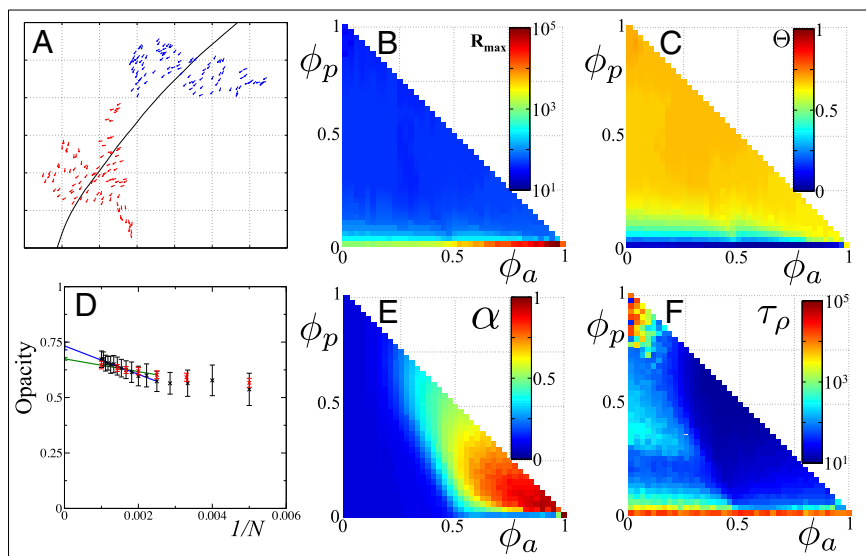


**Fig. 2.** Results from repeated computer simulation of a simple hybrid projection model, parameterized by the strength of the response of each individual to the projection through the swarm that they see ( $\phi_p$ ) and the strength of the alignment with their four nearest neighbors ( $\phi_a$ ). In *B*, *C*, *E*, and *F* (2D), each small colored square (point), corresponding to a pair of parameter values  $\{\phi_a, \phi_p\}$ , is an average value over 400,000 timesteps for  $n = 100$  individuals. (*A*) A snapshot of a swarm in 2D with  $\phi_a = 0.75$  and  $\phi_p = 0.1$  at two different times (blue then red). Its center of mass is moving along the solid line. (*B*) The distance between the two furthest individuals in the swarm,  $R_{max}$ , in units of particle diameter; the swarm does not fragment unless  $\phi_p = 0$ . (*C*) The average opacity  $\Theta$ . (*D*) The average opacity of swarms containing different numbers of individuals  $N$  (the axis shows  $1/N$ ), as seen by internal observers for 2D (black) and 3D (red) swarms, with  $\phi_p = 0.03$  and  $\phi_a = 0.8$  averaged over at least 50,000 timesteps. The linear fit, with an  $R^2$  value of 0.97 for 2D (blue) and 0.99 for 3D (green), is to all data points  $n \geq 400$ . (*E*) The average speed,  $\alpha$ , of the center of mass of the swarm, normalized by the individual's speed; this sometimes is referred to as the order parameter. (*F*) The swarm density autocorrelation time  $\tau_\rho$ , in simulation timesteps. The upper left corner of this panel represents dynamically "jammed" states that we believe are unphysical (see *SI Appendix* for details).

for  $\Theta$  that approach 1 as the number of individuals in a swarm increases; i.e., they always become fully opaque (see *SI Appendix* for details). In such metric-based models, the density of the swarm is fixed by the control parameters. Thus, for any combination of these parameters, there always will be a critical size at which the swarm becomes opaque. For the typical values analyzed in the literature, rather small flocks with  $n < 100$  already are fully opaque (see *SI*

*Appendix* for details). The only possible approach to preventing swarms from becoming opaque with such models would be to modify their control parameters continuously as a function of the swarm size. This would represent a significant proliferation in control parameters from a baseline level that already is typically far higher than in the present work. This is the signature of a class of models that are structurally inadequate to explain marginal opacity.

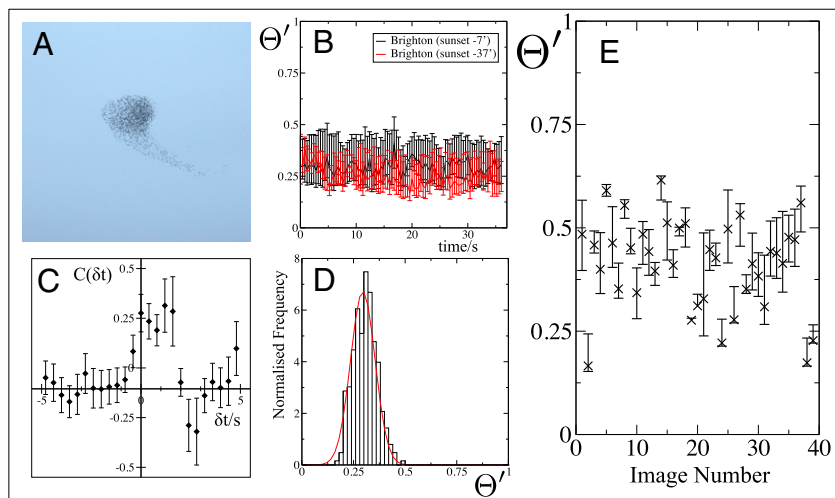


**Fig. 3.** (*A*) A snapshot of a flock of starlings (image contributes to the data presented in *B–D*; see also *Movies S7* and *S8*). (*B*) Typical time variation of the opacity  $\Theta'$  of starling flocks observed in dim light (black) and under brighter conditions (red). (*C*) Cross-correlation function of the horizontal acceleration  $a$  of the center of mass of a flock and its opacity  $C(\delta t)$  as a function of the delay  $\delta t$ . (*D*) Histogram of the opacity  $\Theta'$  of different Starling flocks from across the United Kingdom, corresponding to  $n = 118$  uncorrelated measurements. The red line displays a Gaussian distribution fitted to this data with  $\mu = 0.30$ ,  $\sigma^2 = 0.059$ . (*E*) The opacity  $\Theta'$  of images of starling flocks in the public domain ( $\mu = 0.41$ ,  $\sigma^2 = 0.012$ ). In both *D* and *E*, the null hypothesis that the opacities are drawn from a uniform distribution on  $[X, 1]$  can be rejected at the 99.99% confidence level for all values of  $X$ . These flocks are all marginally opaque. See *SI Appendix* for details throughout.

In Fig. 2 *B*, *C*, *E*, and *F*, we see that individuals do not respond to the projection at all in the narrow strip where  $\phi_p = 0$ . Here the swarm fragments/disperses. Provided there is even a very weak coupling to the projection, i.e.,  $\phi_p > 0$ , the swarm no longer dissipates (see also *SI Appendix*). In Fig. 2*F*, the narrow red strip near  $\phi_p = 0$  shows that the response of the swarm is slow in the absence of the projection term. Here, even when the swarm does not fragment, the dynamics depend on the exchange of information between nearest neighbors. The correlation time decreases as the strength of response to the projection is turned on. This is because the projection provides a global interaction and therefore may lead to rapid dynamic response, consistent with the fast transients observed in real flocks. The nature of this model also makes it robust in response to shocks, such as those caused by predation in real animal systems (*Movies S9* and *S10*). We now compare our model with data on flocks of starlings (Fig. 3).

Datasets for the 3D positions of birds in a flock, such as reported in refs. 1, 5, have given us many new insights, but there are well-known issues associated with particle-tracking techniques in high-density flocks. These issues make using these techniques to obtain unbiased measurements of opacity itself problematic. Instead, we chose to study data for 2D projections, as this was best suited to test our prediction of projected opacity. Fig. 3*B* shows that the opacity remains roughly constant over a period in which the flock reverses direction several times. Fig. 3*C* shows that opacity changes significantly within a few seconds of rapid acceleration and therefore might be implicated in long-range information exchange across the flock. The crucial feature in both Fig. 3*D* (our data) and Fig. 3*E* (public domain images) is that the opacity is intermediate, i.e., neither very close to zero nor unity, despite the fact that the flocks had very different sizes and were observed under different conditions (the flocks we analyzed in Fig. 3 *B–D* generally are smaller than in those in Fig. 3*E*). To our knowledge, this feature is not found in any existing models but emerges naturally from our hybrid projection model.

It is insightful to consider the following simple mean field argument for the consequences of marginal opacity: Consider a randomly chosen line of sight through or out from a typical location near the center of an idealized homogenous, isotropic flock. Because the probability that any small region is occupied is proportional to its volume multiplied by the density of individuals, the probability that a line of sight reveals “sky” is Poisson distributed according to  $P_{sky} \approx e^{-\rho b^d} R^{-1}$  with  $\rho = N/R^d$  a  $d$ -dimensional density,  $b$  the effective linear size of an individual, and  $R$  the linear size of the flock. Our hypothesis of marginal opacity corresponds to  $P_{sky}$  being of order unity (a half, say) leading to  $\rho \sim N^{-1/(d-1)}$ , i.e.,  $\rho \sim N^{-1}$  in 2D and  $\rho \sim N^{-1/2}$  in 3D. Marginal opacity therefore requires that either the density be a decreasing function of  $N$  or that the flock morphology change (or both). There are hints of both these qualities in some published data (1, 5) not inconsistent with the predictions of our model.

Our mean field analysis also may be used to understand why the emergence of marginal opacity is quite a surprising result. It follows that most spatial arrangements of  $N$  finite-sized particles are either opaque ( $\Theta \sim 1$ ) or predominantly transparent ( $\Theta \ll 1$ ).

The latter obviously occurs whenever the density is very low (and in an essentially infinite space, there is plenty of room to achieve this), whereas the former arises even for a relatively small reduction in the separation between individuals from that found in the marginal state. This a result of the extremely strong dependence of  $P_{sky}$  on the flock size  $R$  (in 3D, it varies exponentially with the square of  $R$ ). To illustrate this, we consider the effect of a reduction by half the spacing between individuals and, hence, also  $R$ . Using  $P_{sky} \approx e^{-N(b/R)^2}$  in 3D, we find that this leads to a change in opacity from (say) 50% before to 94% afterward. Thus, the flock becomes almost completely opaque as a consequence of only a halving of the interbird spacing. Similar arguments apply if  $N$  increases at constant  $R$ , and such variations in both density and size are reported in the literature (e.g., ref. 1, table 1), supporting the claim that the marginal opacity apparent in Fig. 3 *B*, *D*, and *E* is a robust emergent feature.

We believe opacity may be related to evolutionary fitness in flocking animals. Dense swarms are thought to give an advantage against predation due to target degeneracy, in which the predator has difficulty distinguishing individual targets (22). Balancing this is the need for the individuals to be aware of the predator so as to execute evasion. In flocks with very high opacity, only a very small fraction of all individuals would be able to see out of the flock and monitor either the first or subsequent approaches of the predator. Individuals in the interior of such a flock could neither see the predator directly nor respond to the behavior of individuals near the edge that were able to see it. Information about the approaches of a predator instead would have to propagate inward, being passed from (the behavior of) neighbor to neighbor, i.e., very much slower than the speed of light, which instead would operate on a clear line of sight. The state of marginal opacity therefore would seem to balance the benefit of compactness (target degeneracy) with information [“many eyes” (23)]. In particular, very little information would be gained by decreasing the opacity beyond a marginal state. Thus, projection-based models that give rise to marginally opaque states would seem to be both cognitively plausible and evolutionarily fit.

Modern humans also need to extract useful information rapidly from high-dimensional datasets. A generic approach to this is to present information through lower-dimensional projections. This approach is reminiscent of the one that we propose has been adopted by flocking animals. Here a  $2dN$ -dimensional phase space, consisting of the spatial coordinates and velocities of all  $N$  members of the flock, is projected onto a simple pattern on a line (2D) or surface (3D). Perhaps the use of such simplifying projections is more widespread in nature than previously suspected?

**ACKNOWLEDGMENTS.** This work was partially supported by the United Kingdom Engineering and Physical Sciences Research Council through the Molecular Organisation and Assembly in Cells and Complexity Doctoral Training Centres (D.J.G.P. and A.M.M., respectively) and Grant EP/E501311/1 (a Leadership Fellowship to M.S.T.). M.S.T. also is grateful for a Joliot-Curie visiting professorship at Ecole Supérieure de Physique et de Chimie Industrielles Paris and the generous hospitality of the Physico-Chimie Théorique group.

1. Ballerini M, et al. (2008) Empirical investigation of starling flocks: A benchmark study in collective animal behavior. *Anim Behav* 76:201–215.
2. King AJ, Sumpter DJ (2012) Murmurations. *Curr Biol* 22(4):R112–R114.
3. Emmerton J, Delius JD (1993) Beyond sensation: Visual cognition in pigeons. *Vision, Brain, and Behavior in Birds*, eds Zeigler HP, Bischof HJ (MIT Press, Cambridge, MA), pp 377–390.
4. Zeigler HP, Bischof HJ (1993) *Vision, Brain, and Behavior in Birds* (MIT Press, Cambridge, MA).
5. Cavagna A, et al. (2010) Scale-free correlations in starling flocks. *Proc Natl Acad Sci USA* 107(26):11865–11870.
6. Ballerini M, et al. (2008) Interaction ruling animal collective behavior depends on topological rather than metric distance: Evidence from a field study. *Proc Natl Acad Sci USA* 105(4):1232–1237.
7. Vicsek T, Czirók A, Ben-Jacob E, Cohen I, Shohet O (1995) Novel type of phase transition in a system of self-driven particles. *Phys Rev Lett* 75(6):1226–1229.
8. Ginelli F, Chaté H (2010) Relevance of metric-free interactions in flocking phenomena. *Phys Rev Lett* 105:168103.
9. Camperi M, Cavagna A, Giardina I, Parisi G, Silvestri E (2012) Spatially balanced topological interaction grants optimal cohesion in flocking models. *Interface Focus* 2(6): 715–725.
10. Bialek W, et al. (2012) Statistical mechanics for natural flocks of birds. *Proc Natl Acad Sci USA* 109(13):4786–4791.
11. Grégoire G, Chaté H, Tu Y (2003) Moving and staying together without a leader. *Physica D* 181:157–170.
12. Reynolds C (1987) Flocks, herds and schools: A distributed behavioral model. *Comput Graph* 21:25–34.
13. D’Orsogna MR, Chuang YL, Bertozzi AL, Chayes LS (2006) Self-propelled particles with soft-core interactions: Patterns, stability, and collapse. *Phys Rev Lett* 96(10): 104302.

14. Couzin ID, Krause J, James R, Ruxton GD, Franks NR (2002) Collective memory and spatial sorting in animal groups. *J Theor Biol* 218(1):1–11.
15. Giardina I (2008) Collective behavior in animal groups: Theoretical models and empirical studies. *HFSP J* 2(4):205–219.
16. Schellinck J, White T (2011) A review of attraction and repulsion models of aggregation: Methods, findings and a discussion of model validation. *Ecol Modell* 222: 1897–1911.
17. Hildenbrandt H, Carere C, Hemelrijk C (2010) Self-organized aerial displays of thousands of starlings: A model. *Behav Ecol* 21:1349–1359.
18. Hemelrijk CK, Hildenbrandt H (2012) Schools of fish and flocks of birds: Their shape and internal structure by self-organization. *Interface Focus* 2(6):726–737.
19. Bhattacharya K, Vicsek T (2010) Collective decision making in cohesive flocks. *New J Phys* 12:093019.
20. Grégoire G, Chaté H (2004) Onset of collective and cohesive motion. *Phys Rev Lett* 92(2):025702.
21. Geisler WS, Albrecht DG (1997) Visual cortex neurons in monkeys and cats: Detection, discrimination, and identification. *Vis Neurosci* 14(5):897–919.
22. Miller RC (1922) The significance of the gregarious habit. *Ecology* 3:122–126.
23. Pulliam HR (1973) On the advantages of flocking. *J Theor Biol* 38(2):419–422.